Effect of Sorbent Type on the Sorption Enhanced Water Gas Shift Process in a Fluidized Bed Reactor

ARTICLE *in* INDUSTRIAL & ENGINEERING CHEMISTRY RESEARCH · SEPTEMBER 2012

Impact Factor: 2.59 · DOI: 10.1021/ie301100y

I&EC research
Industrial & Engineering Chemistry Research

Article

pubs.acs.org/IECR

Effect of Sorbent Type on the Sorption Enhanced Water Gas Shift Process in a Fluidized Bed Reactor

Yang Liu, Zhenshan Li,* Lei Xu, and Ningsheng Cai

Key Laboratory for Thermal Science and Power Engineering of Ministry of Education, Beijing Municipal Key Laboratory for CO_2 Utilization & Reduction, Department of Thermal Engineering, Tsinghua University, Beijing 100084, China

ABSTRACT: The sorption enhanced water gas shift (SEWGS) reaction was proposed to improve CO_2 capture from blast furnace (BF) gas. The CO in the BF gas is first catalyzed to CO_2 on the sorbent surface, with the formed CO_2 then captured by the CaO. This process involves two reactions: the WGS reaction and the CaO carbonation reaction. The WGS reaction is a surface catalytic reaction, while the CaO carbonation is a bulk reaction. This study of the SEWGS reaction in a fluidized bed reactor showed that the sorbent type has an important effect on the SEWGS reaction, with both the CaO and MgO in the sorbent catalyzing the reaction. For calcined limestone, the WGS reaction occurs on the CaO surface with CO_2 sorption in situ, but the reaction rate gradually decreases with the CaO conversion due to coverage by the $CaCO_3$ product layer on the CaO surface. Thus, the shift reaction becomes the rate limiting step. For calcined dolomite, MgO in the sorbent does not react with CO_2 and can then be used as a catalyst. The shift reaction is not a limiting step, with most of the CO_2 for the CaO carbonation coming from the WGS reaction on the MgO surface. Even when the CaO surface is completely covered by the $CaCO_3$ product, the MgO in the calcined dolomite is not completely covered by the $CaCO_3$ product and can still catalyze the WGS reaction. An important phenomenon observed was that not only CaO but also MgO experienced the decay in the catalytic reactivity after multiple cycles. The decay of catalytic reactivity of MgO in dolomite is mainly the gradual covering of the MgO surface by CaO/$CaCO_3$ grains, so most of the MgO grains will lose contact with the CO and the steam in the gas phase. The observation of encapsulation of MgO particles by CaO or $CaCO_3$ is also important for understanding the stabilization of synthetic calcium based sorbent with support addition.

1. INTRODUCTION

CO_2 release from fossil fuel combustion is known to enhance the greenhouse effect with possible disastrous effects due to climate change. CO_2 emissions into the atmosphere have been reported to account for half the greenhouse effect that causes global warming.[1] Besides power plants, other industries are also contributors to anthropogenic CO_2 emissions.[2] The iron and steel sector alone emits about 30% of the total direct industrial CO_2 and nearly 10% of the global total CO_2.[3] In iron and steel plants based on blast furnaces (BFs), about 70% of the CO_2 emissions come from the blast furnace (BF) gas.[4] CO_2 releases from the iron and steel industry can be reduced by CO_2 (or carbon) capture and storage (CCS) from BF gas. The BF gas composition differs greatly from that of flue gas, containing CO_2 (17−25%), CO (20−28%), H_2 (1−5%), and N_2 (50−55%).[5] Therefore, oxyfuel combustion[6] or chemical looping combustion[7] cannot be easily used to capture the CO_2 from BF gas, because about half the BF gas is N_2. Conventional precombustion or postcombustion methods can be used to capture CO_2 in the BF gas, but a greater efficiency penalty is imposed upon these CO_2 emission sources. CaO looping, a recently developed technology, can be used for CO_2 absorption gasification,[8] hydrogen production from integrated coal gasification,[9] sorption enhanced steam methane reforming,[10] sorption enhanced water gas shift reaction,[11] and CO_2 separation from flue gas[12] or syngas.[13] However, little attention has been paid to CO_2 capture from BF gas. In this work, the sorption enhanced water gas shift (SEWGS) reaction based on CaO looping was investigated for CO_2 capture from BF gas, as shown in Figure 1.

The SEWGS process consists of a shift reactor and a regenerator, connected by solid transport lines. The BF gas is introduced into the shift reactor and the following reactions happen:

water gas shift (WGS):

$$CO + H_2O = CO_2 + H_2 \qquad -41.5\ \text{kJ/mol} \tag{1}$$

CO_2 removal:

$$CO_2 + CaO = CaCO_3 \qquad -178\ \text{kJ/mol} \tag{2}$$

The addition of the Ca-based sorbent to the shift reactor removes CO_2 in situ as soon as it is formed, thereby changing the shift reaction equilibrium. Since the shift and carbonation reactions are both exothermic, steam can be produced to generate electricity by immersing the heat transfer surface in the shift reactor. The produced $CaCO_3$ is transported to the regenerator, where the temperature is maintained above 900 °C in pure CO_2 atmosphere or 850−900 °C if steam is used as the purging gas (depending on CO_2 partial pressure), and the decomposition of $CaCO_3$ occurs as follows:

sorbent regeneration:

$$CaCO_3 = CO_2 + CaO \qquad +178\ \text{kJ/mol} \tag{3}$$

Received: April 27, 2012
Revised: July 14, 2012
Accepted: August 24, 2012
Published: August 24, 2012

dx.doi.org/10.1021/ie301100y | *Ind. Eng. Chem. Res.* 2012, 51, 11989−11997

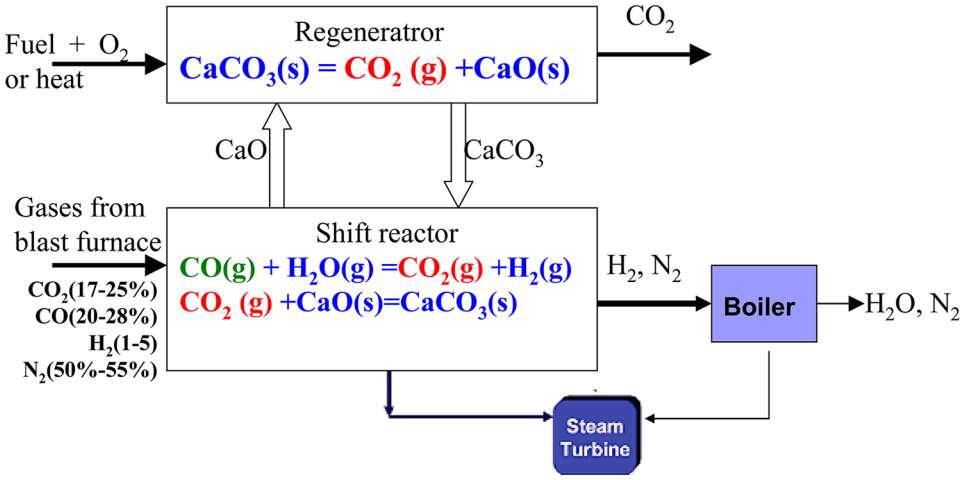

Figure 1. SEWGS process for CO_2 capture from BF gas.

The $CaCO_3$ decomposition is endothermic with the required heat supplied by burning fuels with pure oxygen diluted with CO_2 and steam, thus generating a nearly pure CO_2 stream. In the cyclic mode, the sorbent circulates between a carbonator and a regenerator. Therefore, the sorbent itself is essentially not consumed, but acts as a CO_2 carrier. The outlet gas after the CO_2 removal from the shift reactor contains H_2, N_2, and a small amount of unconverted CO, which will enable higher electrical efficiencies when used for power generation in gas turbines or boilers, as shown in Figure 1.

For CO_2 capture from the BF gas using the SEWGS reaction, the CO contained in the BF gas is converted to CO_2 and then the CO_2 produced by the water gas shift (WGS) reaction is captured by CaO. Therefore, the WGS reaction in the presence of the sorbent is an important step. Some studies have been published about the SEWGS reaction and process development aimed at hydrogen production. Gludd et al.[14] patented the WGS process where Ca-based sorbent is added into the shift reactor. Squires[8] renewed the concept and identified solutions to practical problems associated with the process. Han and Harrison[15] studied the combined shift and carbonation reactions in a single processing vessel. Fan et al.[16] suggested that the SEWGS reaction could simultaneously remove carbon dioxide, sulfur, and chloride impurities at high temperatures during the generation of high-purity hydrogen. Ramkumar et al.[17] investigated H_2 production with contaminant removal in the SEWGS process in the presence of a CaO sorbent and catalyst. The catalyst can have some problems, such as sorbent/catalyst separation before sorbent calcination, catalyst deactivation in the presence of H_2S, and catalyst sintering, so some researchers investigated the SEWGS reaction without a shift catalyst. Harrison and Han[18] studied SEWGS results based on a syngas feed with the addition of dolomite in the absence of a WGS catalyst. Ramkumar et al.[13] also investigated the SEWGS reaction without a catalyst and determined the optimum process conditions for H_2 production in the absence of a catalyst. However, the studies by Harrison and Fan et al. used stainless steel reactors, which were demonstrated to catalyze the WGS reaction. Only a few studies have avoided the catalytic action of the steel reactor. Bretado et al.[19] used a quartz tube fixed bed reactor to study a single WGS step without a catalyst, avoiding the effect of the steel reactor on the WGS reaction. They found that dolomite catalyzed the WGS reaction and the chemical species responsible for the activity in calcined dolomite was possibly the MgO. Duarte de Farias et al.[20] also reported that the presence of MgO increased the activity toward the WGS reaction for the creation of OH groups. Fujimoto[21] compared the Cu and Cu/MgO catalysts and found that the addition of MgO improved activity 2−3 times over using Cu alone. These researchers strongly suggested that the MgO in dolomite had a catalytic effect over the WGS reaction and the CaO carbonation reaction made the WGS exceed the equilibrium limitation. The SEWGS reaction depends on the combination of both WGS and carbonation reactions to improve CO conversion and decrease CO_2 concentration. Therefore, there is a need to compare the catalysis and CO_2 capacities of different nature sorbents. In practical applications, both dolomite and limestone will be repeatedly used. Fluidized beds have also been shown to be suitable for the SEWGS process in CaO looping pilot plant operation experience.[22−25] Therefore, the effect of sorbent type and reactivity decay of the sorbent on the SEWGS reaction in a fluidized bed reactor should be studied in more detail.

The purposes of this study are (1) to study the variation of the product gas evolution profiles with reaction time using five type of sorbents to discern the effect of sorbent type on the SEWGS reaction and (2) to investigate the effect of cycle number on the SEWGS reaction, especially to indentify the mechanism of the sorbent reactivity loss.

2. EXPERIMENT DESCRIPTION

2.1. Fluidized Bed Experiment. The tests were performed in a laboratory-scale bubbling fluidized bed reactor. The fluidized bed apparatus was made of a quartz tube (30 mm i.d., 1200 mm length) supported on a sintered quartz plate as the distributor. The quartz tube was surrounded by an external electrical heater, and the reaction temperature was controlled by only one thermocouple attached to the thermal insulation. The thermocouple measuring bed temperature was not used in order to avoid its possible catalytic activity. It was found that the fluidized bed temperature was lower (~30 °C) than the furnace temperature during the stable operation period. Therefore, from the furnace temperature, we can estimate the bed temperature; the temperature used in the paper is the bed temperature. The flows of CO and N_2 from cylinders controlled by mass flow controllers entered the bottom of the reactor where the gas was preheated by the heating furnace when it flowed upward. The bed material was fluidized by N_2 or the gas

mixture with fine particles in the off-gas filtered by a gravity separation chamber and a piece of quartz wool in the flow path. The reactor outlet was surrounded by heating tape to prevent steam condensation. The CO and CO_2 concentrations in the off-gas were measured continuously by a nondispersive infrared gas analyzer (Signal 9000MGA). The time for complete calcination of the limestone or dolomite was determined when the CO_2 concentration approached zero and the WGS reaction and carbonation time was determined when the reaction came into the postbreakthrough stage. The particles were fully calcinated at 850 °C by N_2 (flow rate 0.89 L(NTP)/min), and then CO (flow rate 0.11 L(NTP)/min) and steam were also introduced into the reactor inlet during the SEWGS reaction at 600 °C. The water flow rate was accurately controlled in the system with a high pressure pump and then evaporated by several heating tapes in the preheating section kept at 180 °C. The steam was then mixed with the gas mixture containing CO and N_2. The experiments used different steam and CO ratios (ranging from 4:1 to 1:2) with a constant CO flow rate. Unless otherwise specified, the steam:CO ratio was 2:1.

2.2. Sorbents. Three limestones and two dolomites from China and the United States were used in this study. One limestone sample was from the district of MiaoFengShan (MFS, limestone), one limestone sample was from NanXinFang (NXF, limestone) and a dolomite sample was from SanCha (SC, dolomite), all in the Yan Mountain area in Beijing. One limestone sample was from the United States (US). One dolomite sample was obtained from HeBei Province of China (HB). The samples were crushed in a crusher and then sieved into a particle size range of 200−500 μm. The sample compositions measured using X-ray fluorescence (XRF) spectrometry (Rigaku ZSX Primus II) are listed in Table 1. Table 1 shows that the CaO and MgO contents of these samples are quite different. The sample mass was about 60 g for each experiment.

Table 1. Sample Compositions (wt %)

composition	US	MFS	NXF	SC	HB
SiO_2	0.67	1.32	2.78	3.88	8.95
Al_2O_3	0.35	0.67	1.55	0.92	1.9
Fe_2O_3	0.11	0.27	0.84	0.29	0.67
CaO	54.38	52.66	39.48	33.21	26.82
MgO	0.74	1.64	7.40	18.60	15.05
K_2O	0.06	0.15	0.16	0.25	0.41
Na_2O	0.09	<0.01	<0.01	<0.01	0.11
MnO	0.003	0.008	0.015	0.012	0.054
TiO_2	0.025	0.02	0.092	0.028	0.067
P_2O_5	0.011	0.231	0.007	0.008	0.066
LOI[a]	43.46	42.95	42.72	42.41	41.54
total	99.89	99.92	95.04	99.61	99.91

[a]Loss on ignition.

3. RESULTS

3.1. Effect of Sorbent Type on the SEWGS Reaction. In the SEWGS step, the ratio of H_2O to CO is an important parameter which affects the CO conversion. If the purpose of the SEWGS system is carbon capture and sequestration, such as shown in Figure 1, the system should convert the maximum possible amount of the CO in the BF gas to CO_2 and improve the CO_2 capture efficiency. Alternatively, if the SEWGS system is used for producing hydrogen or for adjusting the H_2/CO ratio in a chemical plant, such as in Fischer−Tropsch synthesis or methanation with syngas, the system need not completely convert the CO into CO_2. Therefore, the influence of the H_2O fraction on the SEWGS reaction was studied at 600 °C with calcinated limestone as sorbent. The results can be found in Figure 2, where the mole percentages (dry basis) of CO and

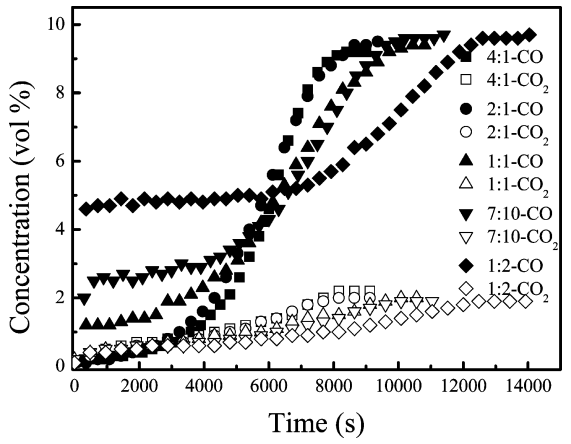

Figure 2. Effect of H_2O/CO ratio on the SEWGS reaction with MFS limestone at 600 °C.

CO_2 in the product gas are plotted versus time, and Figure 2 can be divided into prebreakthrough, breakthrough, and postbreakthrough periods. It can be seen from Figure 2 that the H_2O/CO ratio significantly affects the CO conversion and the prebreakthrough period time. For H_2O/CO ratios of 1:2, 7:10, 1:1, and 2:1, the CO conversion during the prebreakthrough period was about 50, 75, 90, and 95%, with H_2/CO ratios of 1:1, 3:1, 9:1, and 20:1. The prebreakthrough period times were 6000, 4000, 3000, and 2500 s. Thus, the CO conversion and the H_2/CO ratio in the prebreakthrough period of the SEWGS reaction can be controlled by adjusting the H_2O/CO ratio, while during the breakthrough period the CO conversion is not stable and decreases with increasing CaO conversion.

From Figure 2, for H_2O/CO ratios greater than 2, further increases of the steam fraction did not obviously change the SEGWS reaction results; therefore, the H_2O/CO ratio for other experiments was set as 2. The experimental results for the SEWGS reaction with five sorbents are all shown in Figure 3; it can be seen that the sorbent type has an important effect on the SEWGS reaction. For example, just as shown in Figure 3, the CO conversions during the postbreakthrough period are ∼0.5, 1, 15, 30, and 50% for the US, MFS, NXF, SC, and HB samples, respectively. From Table 1, the CaO contents of the US, MFS, NXF, SC, and HB samples are 54.38, 52.66, 39.48, 33.21, and 26.82% while the MgO contents of these sorbents are 0.74, 1.64, 7.4, 18.6, and 15.05%. Therefore, the CO conversion during the postbreakthrough period is related to the MgO content or the CaO content (except for the HB dolomite). The CO conversion during the postbreakthrough period increases with increasing MgO content or decreasing CaO content. At the same time, the CO_2 concentration in the postbreakthrough period increases with increasing MgO content, as shown in Figure 3b. In practical application, the SEWGS reaction mainly happened at the prebreakthrough period to acquire higher CO conversion and decrease CO_2 concentration. Figure 3a shows

dx.doi.org/10.1021/ie301100y | Ind. Eng. Chem. Res. 2012, 51, 11989−11997

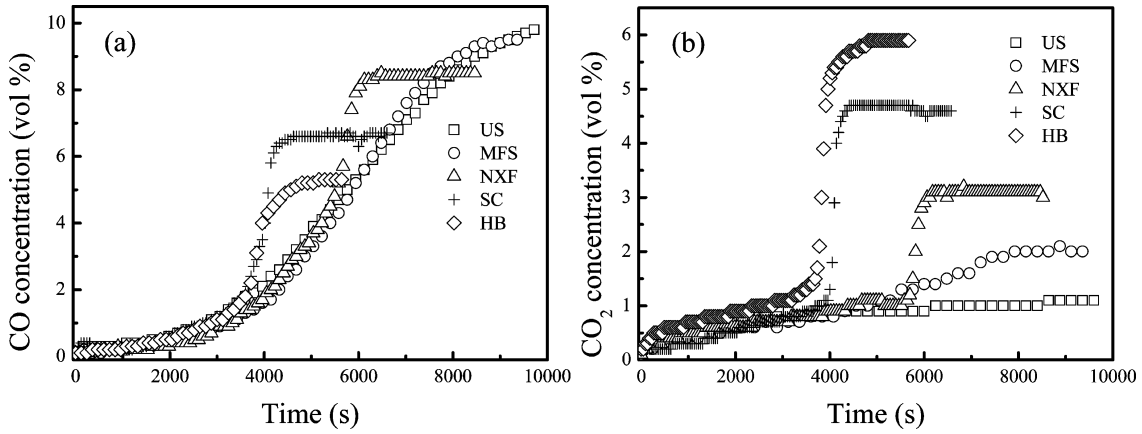

Figure 3. Comparison of gas concentrations at the reactor outlet for different sorbents at 600 °C. (a) CO; (b) CO_2.

that 80% CO conversion is kept for more than 1 h for every kind of sorbent. Comparing the CO and CO_2 concentrations of HB dolomite and US limestone in Figure 3, the reaction using the dolomite still showed higher catalysis than the reaction using the limestone after losing CO_2 adsorption capability. The different CO and CO_2 evolution profiles shown in Figure 3 are assumed to be due to the different catalytic activities of MgO and CaO for the WGS reaction. To validate this assumption, pure MgO and CaO powders were used to check their catalytic reactivities for the WGS reaction. The results (not shown here) indicated that both CaO and MgO can catalyze the WGS reaction. Therefore, the CO conversion during the postbreakthrough period increases with increasing MgO content due to the catalytic reactivity of MgO in the dolomite, as shown in Figure 3.

There are significant differences between the CO and CO_2 evolution profiles in parts a and b of Figure 3 for the different sorbents. For the limestone, there is no obvious breakthrough period for the CO and CO_2 evolution profiles, while the dolomite clearly has the breakthrough and the postbreakthrough periods in the CO and CO_2 evolution profiles. Through integration of CO and CO_2 concentrations with time, it was found that the critical CaO conversions, which indicate the end of the fast carbonation stage and the start of the product layer diffusion stage (also corresponding to the critical product layer thickness[26]), are about 0.85, 0.75, and 0.65 for the HB, SC, and NXF samples. The US and MFS samples see no critical CaO conversions, as shown in Figure 3.

The shift reaction and the CO_2 sorption occur simultaneously on the CaO surface, but the carbonation rate depends on the shift reaction rate because the CO_2 for carbonation comes from the shift reaction. The results shown in Figure 3 show that the CO_2 concentration is always low (Figure 3b for limestone). Thus, the shift reaction is the limiting step for limestone sorbent. The CO shift reaction occurs on the CaO surface; therefore, the CaO surface area is an important parameter. As the reaction time increases, the CaO surface will be gradually covered by $CaCO_3$ product. Thus, the solid product growth mode is also important. The three basic growth modes[27] are (i) island growth, (ii) layer growth, and (iii) island−layer growth. If the solid product growth follows the layer growth mode, the sorbent surface will be rapidly covered by the solid product layer and will rapidly lose its catalytic activity because the CO and H_2O from the gas phase cannot directly contact the sorbent surface. In this case, the WGS reaction occurs through the product layer diffusion which is slow. The island growth mode was observed experimentally[28−30] with the analysis showing that the solid product will grow as a three-dimensional island shape with the solid reactant surface slowly covered by product islands. Therefore, more sorbent surface will be available for direct surface reactions. The CaO surface area will decrease as the CaO conversion increases, so the CO shift rate will gradually decrease. When the CaO surface is completely covered by $CaCO_3$ product, the shift reaction rate depends on the product layer diffusion, which is very slow, as can be seen in Figure 3 (in the postbreakthrough period).

For the SEWGS reaction using calcined dolomite as the sorbent, the shift reaction occurs not only on the CaO surface but also on the MgO surface, with the carbonation reaction occurring between the CaO and the gas phase CO_2. As the reaction time increases, the CaO in the calcined dolomite sorbent will be covered gradually by a layer of $CaCO_3$, with the CaO surface area and the CO shift rate decreasing with increasing CaO conversion. However, the MgO can still contact CO and H_2O, so most of the CO will be catalyzed and converted to CO_2 and H_2 on the MgO surface. Therefore, the shift reaction is not the limiting step. This is quite different from the SEWGS reaction on the calcined limestone surface. When the CaO surface is covered completely by $CaCO_3$ product, the unreacted CaO loses most of its catalytic reactivity and the reaction goes into the product layer diffusion stage, but the MgO in the calcined dolomite is not covered completely by $CaCO_3$ product and can still catalyze the WGS reaction. Therefore, the CO conversion with calcined dolomite is still quite high during the postbreakthrough period.

3.2. Effect of Multiple Carbonation/Calcination Cycles on the SEWGS Process. After the SEWGS reaction, the $CaCO_3$ reaction product must undergo the calcination process to generate CaO for repeated use. The effect of multiple cycles on the SEWGS process using the MFS limestone is shown in Figure 4. The results showed that, with increasing number of cycles, the prebreakthrough time decreased due to the decay of the CaO activity. During the calcination, the CaO coalesced and sintered, so the nascent CaO surface area decreased with increasing residence time, which in turn reduced the CaO conversion.[31−33] The CO_2 concentrations in Figure 4 are low for all cycles, indicating that the loss of catalytic activity was dominant.

Published results for CO_2 capture from flue gas with CaO looping showed that the cyclic reactivity of calcined dolomite was better than that of limestone,[34] because the MgO in

dx.doi.org/10.1021/ie301100y | Ind. Eng. Chem. Res. 2012, 51, 11989−11997

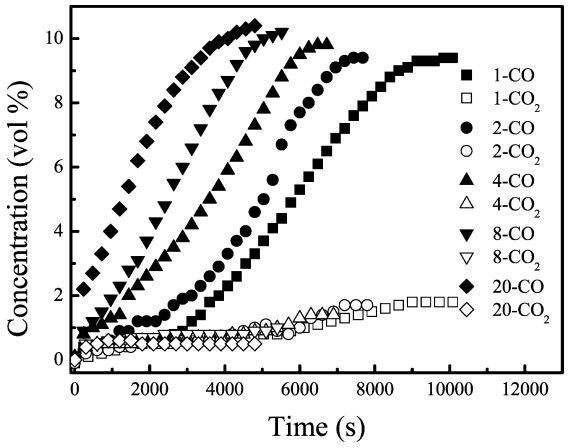

Figure 4. Effect of multiple cycles on the SEWGS reaction using MFS limestone: SEWGS at 600 °C and calcination at 850 °C with nitrogen as the purging gas.

dolomite does not take part in the reaction and can be considered to be inert. The uniform distribution of MgO among the CaO micrograins slowed the sintering of the CaO micrograins during the calcination process. Therefore, the dolomite sorbent was more stable and manifested a high CO_2 adsorption capture.[35] The cyclic SEWGS reaction characteristics using the HB dolomite presented in Figure 5 show that the prebreakthrough time decreases with increasing number of cycles, as with the MFS limestone. At the same time, the CO concentration in the postbreakthrough period increased with the number of cycles, while the CO_2 concentration during the postbreakthrough period decreased.

There are two reactions in the SEWGS process as shown in Figure 1, i.e., the WGS reaction and the CaO carbonation reaction with CO_2. The CO in the BF gas should as much as possible be converted to CO_2. As noted earlier, the sorbent type had an important effect on the WGS reaction. At the same time, the catalytic reactivity decreases with the number of cycles, as shown in Figure 6a, where the ordinate is the total converted CO (including prebreakthrough, breakthrough, and postbreakthrough periods) per unit of sorbent, moles of CO per kilogram of sorbent, used to compare the catalytic reactivity of different sorbents. The results in Figure 6a show that the calcined dolomite has a better cyclic catalytic reactivity than limestone. Besides the catalytic reactivity, the CaO conversion is also an important parameter, because the CO_2 removal is achieved by the CaO carbonation. Figure 6b shows that the cyclic CaO conversion of dolomite is higher than that of limestone. The CaO content in dolomite is lower than that of limestone, so the CaO conversion alone cannot reflect the total amount of captured CO_2 and the sorbent capacity should also be used to compare the sorbent performance. The sorbent capacity is defined as the total amount of captured CO_2 per unit of sorbent, moles of CO_2 per kilogram of sorbent. Theoretically, 56 g of unsupported CaO sorbent should react with 1 mol of CO_2 corresponding to a maximum sorbent capacity of (1 mol of CO_2/kg of CaO)(1000/56) = 17.8 mol of CO_2/kg of sorbent at 100% CaO conversion. Thus, the maximum capacity is 17.8 mol of CO_2/kg of sorbent for all Ca-based sorbents. Figure 6c shows the effect of the number of cycles on the sorbent capacity. The capture CO_2 capacity of limestone is higher than that of dolomite in the first cycles, but the capacity decay of dolomite is less than that of limestone. Thus, selection of the sorbent for the SEWGS process should consider both the cyclic catalytic reactivity and the cyclic sorption capacity to achieve the maximum CO conversion and CO_2 capture.

Figure 7 shows the CO conversion during the postbreakthrough period for different numbers of cycles with the MFS limestone and HB dolomite. The CO conversion during the postbreakthrough period is higher with the dolomite sorbent than with the limestone sorbent because the MgO in the dolomite sorbent still catalyzes the WGS reaction even when the carbonation reaction enters the product layer diffusion controlled stage. An interesting phenomenon is that the CO concentration during the postbreakthrough period decreases continuously with the number of cycles, as shown in Figure 7. For cycle number 20, the CO conversion with the calcined dolomite approaches that of limestone, indicating that most of the MgO in the dolomite has already lost its catalytic reactivity after multiple cycles.

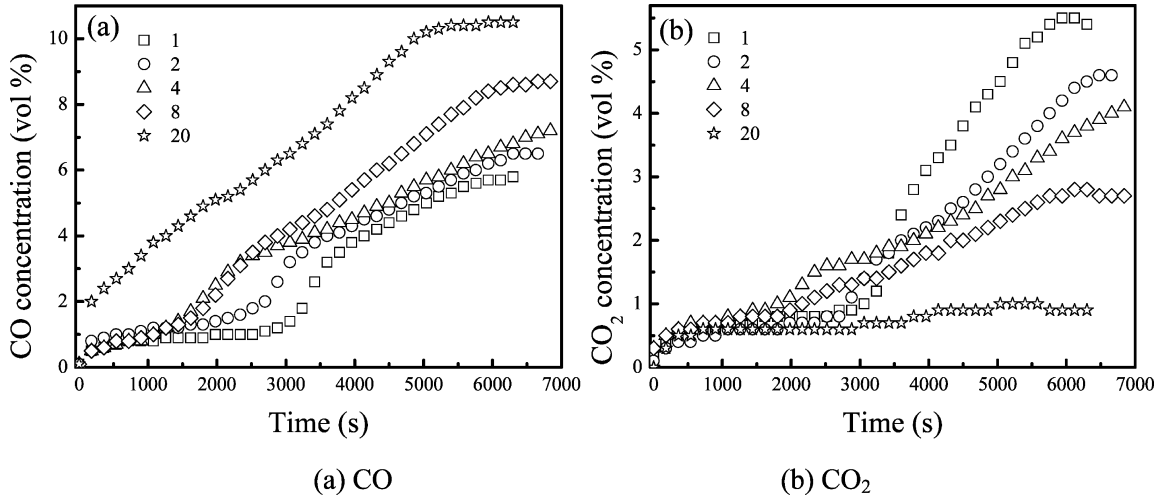

Figure 5. Effect of multiple cycles on the SEWGS reaction using HB dolomite: SEWGS at 600 °C and calcination at 850 °C with nitrogen as the purging gas.

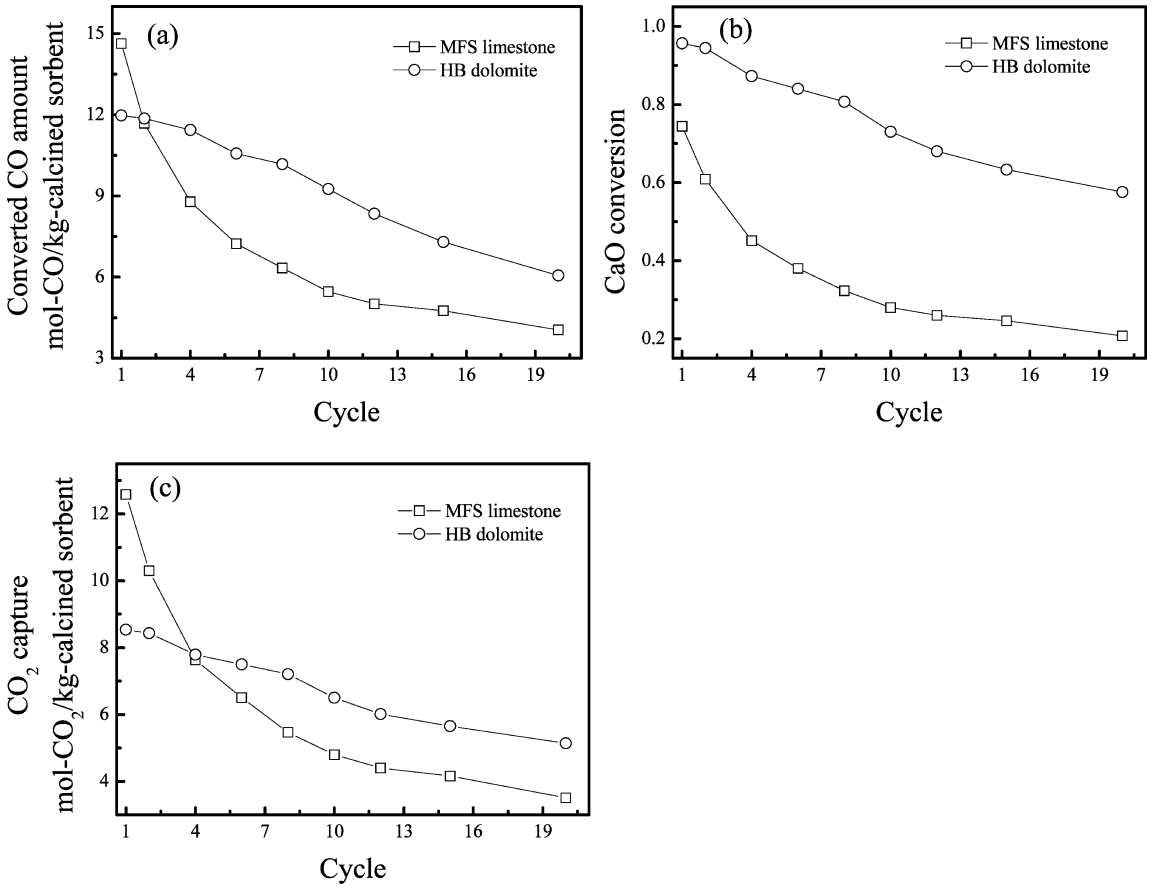

Figure 6. Comparing catalytic reactivity and CO_2 sorption capacity for variant number of cycles using the MFS limestone and the HB dolomite. (a) CO amount catalyzed by calcined sorbent; (b) CaO conversion; (c) CO_2 sorption capacity.

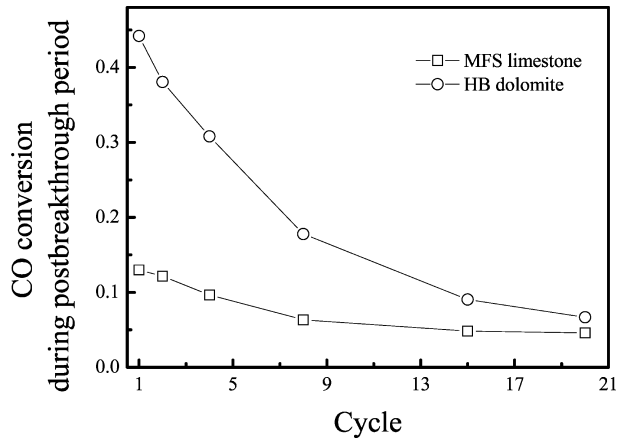

Figure 7. CO conversion during the postbreakthrough period for different numbers of cycles using MFS limestone and HB dolomite.

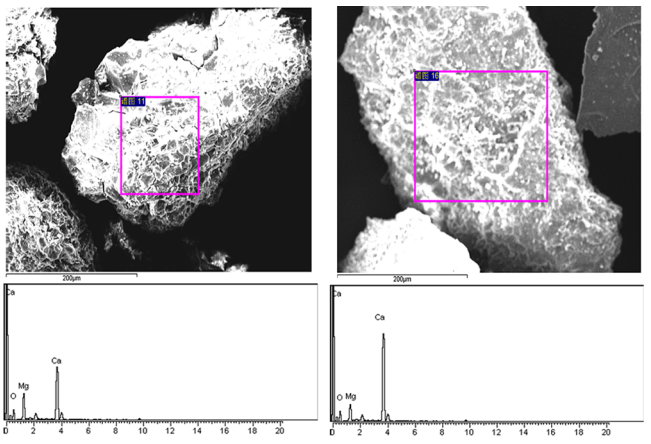

Figure 8. SEM and EDX results of element distribution on dolomite surface for the first calcination (left) and the 20th calcination (right).

4. DISCUSSION

In order to investigate the possible reason for the catalytic activity loss of dolomite, sorbent samples of the first calcination and the 20th calcination were analyzed with scanning electron microscopy (SEM) and energy-dispersive X-ray (EDX) spectrometry, and the results are shown in Figure 8 and Table 2. From the comparison of the distributions of elements on particle surfaces for the first calcination and the 20th calcination, it can be seen clearly that the Mg content (~13%) for the sample after the 20th calcination is much lower than that for the first calcination (~21%). These indicate that part of the MgO on the particle surface may be covered by the CaO grains and lose their surface content during multiple SEWGS/

Table 2. Element Compositions on Particle Surface of Dolomite

	composition (%)					
	O	Mg	Si	Ca	other	total
first calcination	31.02	21.32	4.09	41.78	1.8	100
20th calcination	18.48	13.06	4.87	60.11	3.48	100

dx.doi.org/10.1021/ie301100y | Ind. Eng. Chem. Res. 2012, 51, 11989−11997

calcination cycles. The experimental results in Figure 7, Figure 8, and Table 2 show that not only CaO but also MgO experiences a continuous decay of catalytic reactivity with cycles. A possible mechanism may be the encapsulation of MgO grains.

In the field of calcium looping, it is commonly recognized that the sintering of CaO grains can lead to the decay of reactivity. However, here we provide some insight into the deactivation of MgO catalytic activity under multiple cycles, considering that the encapsulation of MgO grains can make active centers inaccessible to reactants. The encapsulation process can be discussed within the context of the strong metal−support interactions (SMSI) which were first suggested by Tauster et al.[36] to explain the suppression of chemisorption properties on metal particles supported on TiO_2. Later, researchers proposed two kinds of mechanisms to explain the SMSI: a charge transfer mechanism and an encapsulation mechanism.[37] The charge transfer mechanism emphasized the role of chemical bonding which originates from charge transfer between the metal and the oxide, while the encapsulation mechanism explains the loss of catalytic activity due to the partial coverage of metal particles by support material, which blocks active catalytic sites at the metal surface. SMSI were widely observed in many metal/oxide catalytic systems.[38−43]

Two major factors contribute possibly to the encapsulation of MgO grains: a carbonation factor and a CaO sintering factor. As the SEWGS reaction happens on the surfaces of the MgO and CaO grains, the $CaCO_3$ product from the carbonation of CaO with CO_2 will nucleate and grow on the CaO grain surface. It was reported that the $CaCO_3$ product grows as an island shape,[44] and solid state diffusion plays an important role during the carbonation reaction.[45] The formation and growth of the solid product islands associated with $CaCO_3$ solid state diffusion will result in partial coverage of the MgO surface, as shown in Figure 9, so the MgO grains lose part of their catalytic

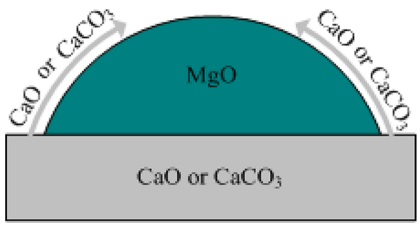

Figure 9. Schematics showing mass migration of CaO or $CaCO_3$ onto MgO.

reactivity. After the SEWGS reaction step, a calcination step is required to regenerate the CaO. This calcination step will start at a higher calcination temperature, causing the CaO grains to diffuse along the MgO grains. This may lead to part of the MgO grains being encapsulated inside CaO grains, as shown in Figure 9, so that these MgO grains lose direct contact with the CO and steam in the gas phase and, therefore, cannot catalyze the WGS reaction. The driving force of this encapsulation of MgO grains by CaO or $CaCO_3$ is the minimization of the surface energy of the system.

In the first cycle, as the natural dolomite is calcined, grains of CaO and MgO will be produced with some pore networks formed between grains,[46] and some MgO grains will adhere to the surface of CaO grain, as shown in Figure 10a. After multiple cycles, the MgO grain surfaces will be gradually covered by CaO or $CaCO_3$ grains (as shown in Figure 10b) so that the MgO cannot directly contact the CO and steam in the gas phase which, therefore, gradually lose their catalytic action for the WGS reaction. Finally, almost all MgO grains are encapsulated by CaO or $CaCO_3$ grains, as shown in Figure 10c; thus, MgO will lose most of its catalytic activity toward the WGS reaction after long repeated cycles due to its encapsulation by CaO grains, as shown in Figure 7.

The above finding of the encapsulation of MgO grains by CaO or $CaCO_3$ is also useful for understanding the interaction between CaO grains and inert support in synthetic calcium based sorbents. The decay of sorbent reactivity is the key problem for the practical progress of the calcium looping concept. The idea of introducing dispersed inert support particles into CaO grains was reported as an effective way to stabilize the cyclic reactivity of CaO.[47] The reason for the stable reactivity of synthesized sorbents such as CaO/$Ca_{12}Al_{14}O_{33}$,[48] CaO/MgO,[49] etc. was attributed to uniform distributed inert support particles such as $Ca_{12}Al_{14}O_{33}$, MgO, etc. which are stable and inhibit or slow the sintering of CaO. The interaction between CaO grains and support particles is critical for the inhibition of CaO sintering, and it is related to the volume fraction (f) of support particles on the CaO grain boundary. It should be noted that the encapsulation of support particles is very important for synthetic sorbents because it changes the geometry of interaction between the support particles and the CaO grain boundary and, therefore, the distribution of support particles on the CaO boundary, finally resulting in the decrease of f (Figure 10) and the reactivity of synthetic sorbents. The experimental results presented in this work provided the evidence of the encapsulation of MgO grains. Another contribution of this work is that the characteristic of the encapsulation of MgO grains during multiple carbonation/calcination cycles can be investigated with the SEWGS experiments, and we believe this method can also be used to test the interaction of CaO with other supports such as CuO and Fe_2O_3.

5. CONCLUSIONS

Calcium oxide is a catalyst for the WGS reaction with in situ CO_2 sorption, and the WGS reaction on the CaO surface is the rate limiting step for SEWGS. The CaO conversion directly affects the WGS reaction rate on the CaO surface. Increasing the CaO conversion reduces the available CaO surface area for the WGS reaction due to the product layer covering the surface, resulting in a gradual reduction of the WGS reaction rate. For sorbents containing MgO, both CaO and MgO act as catalysts, so the shift reaction is not the limiting step with most of the CO_2 for the carbonation of CaO coming from the WGS reaction on the MgO surface. When the CaO surface is covered completely by $CaCO_3$ product, the MgO in the calcined dolomite is not covered by $CaCO_3$ product and can still catalyze the WGS reaction. The MgO in dolomite will also experience some decay of catalytic activity, mainly due to the encapsulation and blockage of active site by the migration of the CaO or $CaCO_3$ grains. During multiple cycles, the MgO surface will be gradually covered by CaO or $CaCO_3$ grains, and finally most MgO grains lose direct contact with the CO and steam in the gas phase, therefore resulting in the loss of catalytic activity. The observation of encapsulation of MgO grains is important for understanding the mechanism of reactivity loss for some sorbents such as dolomite and synthetic sorbents.

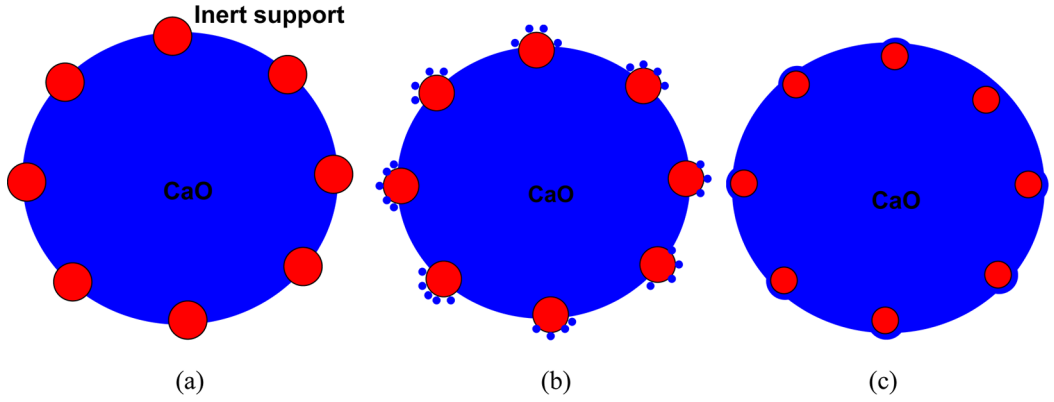

Figure 10. Possible mechanism for reactivity loss of dolomite during repeated SEWGS/calcination cycles. (a) Initial state between CaO and MgO; (b) partial encapsulation of MgO; (c) complete encapsulation of MgO.

AUTHOR INFORMATION

Corresponding Author

*Tel.: 86-10-62789955. Fax: 86-10-62770209. E-mail: lizs@tsinghua.edu.cn.

Notes

The authors declare no competing financial interest.

ACKNOWLEDGMENTS

This research was supported by the National Natural Science Funds of China (No. 51061130535) and by the National Basic Research Program of China (No. 2011CB707301).

REFERENCES

(1) Houghton, J. T.; Filho, L. G. M. In *Climate Change 1995: The Science of Climate Change, Contribution of Working Group I to the Second Assessment Report of the Intergovernmental Panel on Climate Change*; Cambridge University Press: Cambridge, U.K., 1996.

(2) IEA. *Energy Technology Transitions for Industry—Strategies for the Next Industrial Revolution*; International Energy Agency: Paris, France, 2009.

(3) IEA. *Tracking Industrial Energy Efficiency and CO_2 Emissions*; International Energy Agency: Paris, France, 2008.

(4) Farla, J. C. M.; Hendriks, C. A.; Blok, K. Carbon dioxide recovery from industrial processes. *Clim. Change* **1995**, *29*, 439−461.

(5) IPPC. *Reference Document on Best Available Techniques on the Production of Iron and Steel*; Integrated Pollution Prevention and Control Bureau: Seville, Spain, 2001.

(6) Chen, L.; Yong, S. Z.; Ghoniem, A. F. Oxy-fuel combustion of pulverized coal: Characterization, fundamentals, stabilization and CFD modeling. *Prog. Energy Combust. Sci.* **2012**, *38*, 156−214.

(7) Adanez, J.; Abad, A.; Garcia-Labiano, F.; Gayan, P.; Diego, L. F. d. Progress in Chemical-Looping Combustion and Reforming technologies. *Prog. Energy Combust. Sci.* **2012**, *38*, 215−282.

(8) Squires, A. M. Cyclic use of calcined dolomite to desulfurize fuels undergoing gasification. *Adv. Chem. Ser.* **1967**, *25*, 205.

(9) Lin, S. Y.; Suzuki, Y.; Hatano, H.; Harada, M. Developing an innovative method, HyPr-RING, to produce hydrogen from hydrocarbons. *Energy Convers. Manage.* **2002**, *43*, 1283−1290.

(10) Harrison, D. P. Sorption-enhanced hydrogen production: A review. *Ind. Eng. Chem. Res.* **2008**, *47*, 6486−6501.

(11) Muller, C. R.; Pacciani, R.; Bohn, C. D.; Scott, S. A.; Dennis, J. S. Investigation of the enhanced water gas shift reaction using natural and synthetic sorbents for the capture of CO_2. *Ind. Eng. Chem. Res.* **2009**, *48*, 10284−10291.

(12) Blamey, J.; Anthony, E. J.; Wang, J.; Fennell, P. S. The calcium looping cycle for large-scale CO_2 capture. *Prog. Energy Combust. Sci.* **2010**, *36*, 260−279.

(13) Ramkumar, S.; Fan, L. S. Calcium looping process (CLP) for enhanced noncatalytic hydrogen production with integrated carbon dioxide capture. *Energy Fuels* **2010**, *24*, 4408−4418.

(14) Gluud, W.; Keller, K.; Schonfelder, R.; Klempt, W. *Production of Hydrogen*. U.S. Patent 1,816,523, 1931.

(15) Han, C.; Harrison, D. P. Simultaneous shift reaction and carbon dioxide separation for the direct production of hydrogen. *Chem. Eng. Sci.* **1994**, *49*, 5875−5883.

(16) Fan, L.; Li, F.; Ramkumar, S. Utilization of chemical looping strategy in coal gasification processes. *Particuology* **2008**, *6*, 131−142.

(17) Ramkumar, S.; Iyer, M. V.; Fan, L. S. Calcium looping process for enhanced catalytic hydrogen production with integrated carbon dioxide and sulfur capture. *Ind. Eng. Chem. Res.* **2011**, *50*, 1716−1729.

(18) Harrison, D.; Han, C.; Lee, G. A calcium oxide sorbent process for bulk separation of carbon dioxide. Presented at the Advanced Coal-Fired Power Systems '95 Review Meeting, Morgantown, WV, 1995.

(19) Bretado, M. A. E.; Vigil, M. D. D.; Gutierrez, J. S.; Ortiz, A. L.; Collins-Martinez, V. Hydrogen production by absorption enhanced water gas shift (AEWGS). *Int. J. Hydrogen Energy* **2010**, *35*, 12083−12090.

(20) Duarte de Farias, A. M.; Barandas, A. P. M. G.; Perez, R. F.; Fraga, M. A. Water-gas shift reaction over magnesia-modified Pt/CeO_2 catalysts. *J. Power Sources* **2007**, *165*, 854−860.

(21) Fujimoto, K. New Uses of Methane. In *Natural Gas Conversion II*; Curry-Hyde, H., Howe, R., Eds.; Studies in Surface Science and Catalysis 81; Elsevier: Amsterdam, The Netherlands, 1994; pp 73−84.

(22) Alonso, M.; Rodriguez, N.; Gonzalez, B.; Grasa, G.; Murillo, R.; Abanades, J. C. Carbon dioxide capture from combustion flue gases with a calcium oxide chemical loop. Experimental results and process development. *Int. J. Greenhouse Gas Control* **2010**, *4*, 167−173.

(23) Charitos, A.; Hawthorne, C.; Bidwe, A. R.; Sivalingam, S.; Schuster, A.; Spliethoff, H.; Scheffknecht, G. Parametric investigation of the calcium looping process for CO_2 capture in a 10 kW dual fluidized bed. *Int. J. Greenhouse Gas Control* **2010**, *4*, 776−784.

(24) Fang, F.; Li, Z. S.; Cai, N. S. Continuous CO_2 capture from flue gases using a dual fluidized bed reactor with calcium-based sorbent. *Ind. Eng. Chem. Res.* **2009**, *48*, 11140−11147.

(25) Gonzalez, B.; Alonso, M.; Abanades, J. C. Sorbent attrition in a carbonation/calcination pilot plant for capturing CO_2 from flue gases. *Fuel* **2010**, *89*, 2918−2924.

(26) Alvarez, D.; Abanades, J. C. Determination of the critical product layer thickness in the reaction of CaO with CO_2. *Ind. Eng. Chem. Res.* **2005**, *44*, 5608−5615.

(27) Bechstedt, F. *Principles of Surface Physics*; Springer-Verlag: Berlin, 2003; pp 60−63.

(28) Fang, F.; Li, Z. S.; Cai, N. S.; Tang, X. Y.; Yang, H. T. AFM investigation of solid product layers of $MgSO_4$ generated on MgO surfaces for the reaction of MgO with SO_2 and O_2. *Chem. Eng. Sci.* **2011**, *66*, 1142−1149.

(29) Li, Z. S.; Fang, F.; Cai, N. S. Characteristic of solid product layer of $MgSO_4$ in the reaction of MgO with SO_2. *Sci. China: Technol. Sci.* **2010**, *53*, 1869−1876.
(30) Tang, X.; Li, Z.; Fang, F.; Cai, N.; Yang, H. AFM investigation of the morphology of $CaSO_4$ product layer formed during direct sulfation on polished single-crystal $CaCO_3$ surfaces at high CO_2 concentrations. *Proc. Combust. Inst.* **2011**, *33*, 2683−2689.
(31) Grasa, G. S.; Abanades, J. C. CO_2 capture capacity of CaO in long series of carbonation/calcination cycles. *Ind. Eng. Chem. Res.* **2006**, *45*, 8846−8851.
(32) Manovic, V.; Anthony, E. J.; Grasa, G.; Abanades, J. C. CO_2 looping cycle performance of a high-purity limestone after thermal activation/doping. *Energy Fuels* **2008**, *22*, 3258−3264.
(33) Sun, P.; Lim, J.; Grace, J. R. Cyclic CO_2 capture by limestone-derived sorbent during prolonged calcination/carbonation cycling. *AIChE J.* **2008**, *54*, 1668−1677.
(34) Silaban, A.; Narcida, M.; Harrison, D. P. Characteristics of the reversible reaction between CO_2 and calcined dolomite. *Chem. Eng. Commun.* **1996**, *146*, 149−162.
(35) Dobner, S.; Sterns, L.; Graff, R. A.; Squires, A. M. Cyclic calcination and re-carbonation of calcined dolomite. *Ind. Eng. Chem. Process Des. Dev.* **1977**, *16*, 479−486.
(36) Tauster, S. J.; Fung, S. C.; Garten, R. L. Strong metal-support interactions—group-8 noble-metals supported on TiO_2. *J. Am. Chem. Soc.* **1978**, *100*, 170−175.
(37) Fu, Q.; Wagner, T. Interaction of nanostructured metal overlayers with oxide surfaces. *Surf. Sci. Rep.* **2007**, *62*, 431−498.
(38) Fu, Q.; Wagner, T.; Olliges, S.; Carstanjen, H. D. Metal−oxide interfacial reactions: Encapsulation of Pd on TiO_2(110). *J. Phys. Chem. B* **2005**, *109*, 944−951.
(39) Tauster, S. J.; Fung, S. C.; Baker, R. T. K.; Horsley, J. A. Strong interactions in support-metal catalysts. *Science* **1981**, *211*, 1121−1125.
(40) Bell, A. T. The impact of nanoscience on heterogeneous catalysis. *Science* **2003**, *299*, 1688−1691.
(41) Dulub, O.; Hebenstreit, W.; Diebold, U. Imaging cluster surfaces with atomic resolution: The strong metal−support interaction state of Pt supported on TiO_2(110). *Phys. Rev. Lett.* **2000**, *84*, 3646−3649.
(42) Lewandowski, M.; Sun, Y. N.; Qin, Z. H.; Shaikhutdinov, S.; Freund, H. J. Promotional effect of metal encapsulation on reactivity of iron oxide supported Pt catalysts. *Appl. Catal., A: Gen.* **2011**, *391*, 407−410.
(43) Qin, Z. H.; Lewandowski, M.; Sun, Y. N.; Shaikhutdinov, S.; Freund, H. J. Encapsulation of Pt nanoparticles as a result of strong metal-support interaction with Fe_3O_4 (111). *J. Phys. Chem. C* **2008**, *112*, 10209−10213.
(44) Li, Z. S.; Fang, F.; Tang, X. Y.; Cai, N. S. Effect of temperature on the carbonation reaction of CaO with CO_2. *Energy Fuels* **2012**, *26*, 2473−2482.
(45) Li, Z. S.; Sun, H. M.; Cai, N. S. Rate equation theory for the carbonation reaction of CaO with CO_2. *Energy Fuels* **2012**, *26*, 4607−4616.
(46) Dennis, J. S.; Pacciani, R. The rate and extent of uptake of CO2 by asynthetic, CaO-containing sorbent. *Chem. Eng. Sci.* **2009**, *64*, 2147−2157.
(47) Li, Z. S.; Cai, N. S.; Huang, Y. Y.; Han, H. J. Synthesis, experimental studies, and analysis of a new calcium-based carbon dioxide absorbent. *Energy Fuels* **2005**, *19*, 1447−1452.
(48) Li, Z. S.; Cai, N. S.; Huang, Y. Y. Effect of preparation temperature on cyclic CO_2 capture and multiple carbonation-calcination cycles for a new Ca-based CO_2. sorbent. *Ind. Eng. Chem. Res.* **2006**, *45*, 1911−1917.
(49) Liu, W.; Feng, B.; Wu, Y.; Wang, G.; Barry, J.; da Costa, J. C. D. Synthesis of sintering-resistant sorbents for CO_2 capture. *Environ. Sci. Technol.* **2010**, *44*, 3093−3097.